

## Original Article

# The relationship between MRI and histology in a rat model of intervertebral disc degeneration

Jianming Hua<sup>1</sup>, Yiqing Tao<sup>2</sup>, Xiaopeng Zhou<sup>2</sup>, Gang Chen<sup>2</sup>, Minming Zhang<sup>1</sup>, Fangcai Li<sup>2</sup>, Biao Jiang<sup>1</sup>, Chengzhen Liang<sup>2</sup>

<sup>1</sup>Department of Radiology, 2<sup>nd</sup> Affiliated Hospital, School of Medicine, Zhejiang University, #88 Jiefang Road, Hangzhou, Zhejiang, China; <sup>2</sup>Department of Orthopedics, 2<sup>nd</sup> Affiliated Hospital, School of Medicine, Zhejiang University, #88 Jiefang Road, Hangzhou, Zhejiang, China

Received January 9, 2016; Accepted May 18, 2016; Epub July 15, 2016; Published July 30, 2016

**Abstract:** Objectives: To establish a slowly progressive, reproducible rat model of disc degeneration and investigate the relationship between MRI and histology in the long-term progression of disc degeneration. Materials and methods: The intervertebral discs of caudal spine in rats were punctured laterally, using 20-gauge sterile needles, 5 mm depth from the skin to the middle of the appropriate disc. The discs of tails were analyzed by *in vivo* MRI and histology before surgery and at 4, 8, 12, and 24 weeks post-surgery. Results: Based on histological grading system, the discs were categorized as normal, moderately degenerated, and severely degenerated, and histologic score of treatment groups was significantly correlated with the time post-stab. MRI measurements showed a progressive decrease in T2 signal intensity and MRI index starting at 4 weeks post-puncture. Furthermore, the degenerated discs did not recover spontaneously, as shown by decrease in T2 signal intensity and MRI index. We found significant correlation between the grade scale of histological score and MRI measurements. Conclusions: We demonstrated a correlation between grade scale of histological score and MRI measurements in a slow and progressive disc degeneration rat model. Therefore, MRI could provide a convenient, non-invasive, reproducible, and cost-effective option to monitor the progression of intervertebral disc degeneration.

**Keywords:** Intervertebral disc degeneration, rat, MRI, MRI index, histological score

## Introduction

Low back pain is a major health problem, which leads to disability that reduces the quality of life of the patients and causes costs for medical treatment [1, 2]. Intervertebral disc degeneration (IDD) related diseases are the main reasons of low back pain [3]. Intervertebral disc (IVD) is a cartilaginous tissue that consists of a nucleus pulposus (NP), an annulus fibrosus (AF), and endplates (EP). Although the pathogenesis of IDD remains elusive, some studies have indicated that IDD involves the reduction of disc cells and the extracellular matrix, which consists predominantly of proteoglycans, collagens, and noncollagenous proteins [4, 5]. IDD may increase the range of motion on the adjacent vertebral segments [6].

Recent advancements in molecular biology and tissue engineering have made it possible to directly treat the intervertebral disc at molecular, cellular, and tissue levels to alter the course

of IDD. A number of novel therapeutic approaches have been proposed for IDD, including growth factor therapy, gene therapy, cell therapy, and tissue engineering [7-12]. However, the development of effective therapy requires improved understanding of the pathogenesis and of IDD and rigorous demonstration of the safety and efficacy in suitable animal models that mimic the specific aspects of human IDD [13].

Stab incision at the IVD to induce degeneration has become a widely used *in vivo* model to investigate experimental IVD degeneration and test the effectiveness of new treatments [14, 15]. These perturbations can produce morphologically and biochemically altered features similar to many of those found in human degenerative discs. The classic stab model were widely used in previous studies [16, 17], in which a surgical blade was used to make a transverse stab incision into 2 noncontiguous discs (E.g. L2-L3 and L4-L5) through the rabbit

## Relationship between MRI and histology in disc degeneration

ventral annulus. 20-gauge hypodermic needle is another choice to establish a stab model, which could avoid excessive exposure of surrounding ligaments and tissues that might result in postoperative spur formation. In comparison, needle puncture induces slower and progressive disc degeneration and better represents IDD in human, and thus is suitable for evaluating the effectiveness of new treatments [18]. To date, the needle-puncture model has been established in rabbits and rats [19, 20]. Rodents are attractive models for disc repair because of low cost and ease of care.

Magnetic resonance imaging (MRI) has been widely applied for the detection of earlier IVD degeneration. The signal reduction of the disc on a T2-weighted image reflects a decrease of both proteoglycans and the water content in the disc, and MRI is generally regarded as a sensitive method for evaluating pathological characteristics [21]. While control contact disc showed homogenous, bright NP, and clear distinction between NP and AF, progressive decreases in NP area and signal intensity were apparent for each of punctured discs at 3 weeks post-stab. Moreover, irregular shape of anterior margin of disc suggested early cartilaginous osteophytes at 6 weeks post-stab. At 12 weeks post-stab, irregular shape of NP and dark signal were detected outside anterior AF (osteophyte). At 24 weeks post-stab, extensive decrease in NP area and signal intensity, and increased dark signal outside anterior AF (osteophyte) were observed [22].

To better monitor the long-term progression of IDD with noninvasive MRI, it is important to establish the correlation between histopathologic grading of degenerated discs and MRI measurement. In the present study, a variation of the classic stab model was presented in which the rat caudal disc was stabbed to a limited depth by a 20-gauge hypodermic needle to achieve less precipitous changes in the NP and AF and better mimic early IDD. Based on this model, we performed serial MRI scans and histological analysis to follow the course of IVD degeneration quantitatively up to 24 weeks post-surgery.

### Materials and methods

#### *Experimental animals*

All experimental protocols were approved by the Institutional Animal Care and Use Commi-

tee of Zhejiang University. A total of 48 Sprague-Dawley rats (three months old, 450 g weight) were obtained from the Animal Center of the Academy of Medical Science of Zhejiang Province. Among them, four rats were killed promptly to provide intact disc specimens to indicate the preoperative state of discs. Experiments were performed on the remaining 44 rats as follows.

#### *Surgical technique*

The surgical procedure was performed as described previously [19]. Briefly, 44 male rats were injected intraperitoneally with 1% pentobarbital sodium (Sigma Aldrich, St. Louis, MO, USA) at a dose of 0.4 mL/kg body weight. The intervertebral space was located by digital palpation on the coccygeal (Co) vertebrae and the disc position was labeled using marker pen, and confirmed or corrected by a trial radiograph. After imaging, 44 male rats were randomly divided into two groups: control group and stab group. Then tail skin of stab group was sterilized and a 20-gauge sterile needle was inserted 5 mm depth from the skin to the middle of the appropriate disc, controlled by the handmade stopper [18], through the AF into the NP of Co7/Co8 (between Co7 and Co8) and Co8/Co9 (between Co8 and Co9), rotated 360°, and held for 30 seconds. Throughout all procedures, care was taken to not disturb the periosteal tissues of the vertebrae. Following surgery, the rats were permitted free cage activity (3000 cm<sup>2</sup>), food, and water. The rats were followed serially by MRI for up to 24 weeks, with MRI scans taken before surgery and at 4, 8, 12, and 24 weeks post-surgery. At each of these time points, five rats were killed for histology.

#### *MRI scanning procedures and processing*

At 4, 8, 16 and 24 weeks after operation, the approached caudal spine levels were assessed by MRI. MRI scans were obtained using a 3.0 T MRI scanner (Signa Excite, General Electric Medical Systems) furnished with GE ADW4.2 workstation. Briefly, to obtain T2-weighted sections in the sagittal plane, rats were anesthetized and laid in an animal special coil in the prone position with their tails straight using the following parameter settings of sagittal and axial plane images: spin echo repetition time, 2275 ms and 1780 ms; echo time, 80 ms and 20 ms; field of view, 5 cm; slice thickness, 1.5 mm; spacing, 0 mm; no phase wrap; echo train

## Relationship between MRI and histology in disc degeneration

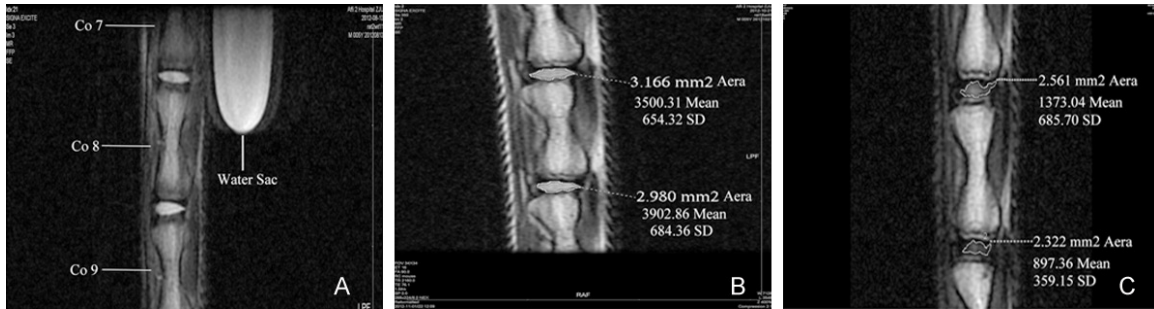


**Figure 1.** The Schematic diagram of measured area of interest in NP, mean signal intensity, and standard derivation.

**Table 1.** Histological grading scale

Histological grading of the disc degeneration seen from inner annulus structure

### *I. Cellularity of the anulus fibrosus*

Grade:

1. Fibroblasts comprise more than 75% of the cells
2. Neither fibroblasts nor chondrocytes comprise more than 75% of the cells
3. Chondrocytes comprise more than 75% of the cells

### *II. Morphology of the anulus fibrosus*

Grade:

1. Well-organized collagen lamellae without ruptured or serpentine fibers
2. Inward bulging, ruptured or serpentine fibers in less than one third of the annulus
3. Inward bulging, ruptured or serpentine fibers in more than one third of the annulus

### *III. Border between the anulus fibrosus and nucleus pulposus*

Grade:

1. Normal, without any interruption
2. Minimal interruption
3. Moderate or severe interruption

### *IV. Cellularity of the nucleus pulposus*

Grade:

1. Normal cellularity with stellar shaped nuclear cells evenly distributed throughout the nucleus
2. Slight decrease in the number of cells with some clustering
3. Moderate or severe decrease (> 50%) in the number of cells with all the remaining cells clustered and separated by dense areas of proteoglycans

### *V. Morphology of the nucleus pulposus*

Grade:

1. Round, comprising at least half of the disc area in midsagittal sections
2. Rounded or irregularly shaped, comprising one quarter to half of the disc area in midsagittal sections
3. Irregularly shaped, comprising less than one quarter of the disc area in midsagittal sections

The scale is based on 5 categories of degenerative changes with scores ranging from 5 points (1 in each category) for a normal disc to 15 points (3 in each category) for a severely degenerated disc.

length, 16 and 4; band width, 41.76 and 10.42; number of excitations, 8; matrix, 288 × 224; Scan Time, 4:18 and 5:26.

Quantitative analysis of the midsagittal image slices was processed using GE ADW4.2 workstation and the intact and stabbed discs were

analyzed qualitatively for evidence of degenerative changes. Four rats in every group were seduced to sleep by pentobarbital sodium for radiological examinations at every time point, and then recovered for other examinations. All image assessments were conducted by three independent, blinded observers. Quantitative

## Relationship between MRI and histology in disc degeneration

**Table 2.** The mean histologic score of moderately or severely degenerated disc in rat

Group (No. of discs)	Time Post-stab (Week)	Histologic score (5-16)
Control disc (40)	12 ± 7.6	5.5 ± 0.51
Moderately degenerated disc (16)	5.5 ± 2	8 ± 1.9†,‡
Severely degenerated disc (24)	16.33 ± 6.76	13.7 ± 1.08†

Values are expressed as the mean ± SD. †P < 0.001 compared with the control disc at the same time point. ‡P < 0.001 moderately degenerated disc compared with severely degenerated disc.

analysis of these images was performed as follows. The NP of each disc was outlined on screen to define the region of interest (ROI), as shown in **Figure 1**. The area and average signal intensity (gray scale value) of the ROI were then computed automatically using the GE ADW4.2 workstation, and the data were downloaded to a computer spreadsheet for analysis. MRI index (the area of NP multiplied by average signal intensity) proposed by Sobajima et al. [22] was used to assess the alteration of the NP. An additional MRI outcome measure “MRI index” (the product of nucleus pulposus area and average signal intensity) was computed to serve as a comprehensive measurement of nucleus pulposus degenerative changes [22].

### Histopathologic analysis

The rats were sacrificed by intraperitoneal injection of 10% chloral hydrate and the tails were harvested at 4, 8, 16 and 24 weeks post-surgery. Specimens were fixed in 10% neutral-buffered formalin, dehydrated, decalcified and embedded in paraffin. The tissues were cut into 5 µm sections. Two slides of each disc were stained with hematoxylin and eosin (H&E). The cellularity and morphology of NP, AF, and EP were examined by two experienced pathologists independently in a blinded fashion, and evaluated by using a grading scale (**Table 1**) as described previously [19, 23]. The histologic score was 5 to 6 for normal disc, 7 to 11 for moderately degenerated disc, and 12 to 14 for severely degenerated disc.

### Statistical analysis

The statistical significance of the differences among the groups in histologic score, T2 intensity and MRI index was assessed using a One-way analysis of variance (ANOVA), followed by post-hoc analysis with Dunnett's T3 test.

All statistical analyses were performed using the SPSS software (16.0; SPSS, Inc. Chicago, IL, USA). P values were two-tailed and a value < 0.05 was considered statistical significance.

## Results

### The survival of the rats

In the present study, four rats (two rats in each group) died due to anesthesia accident, the left 20 rats in each group tolerated the surgery well, with no postoperative behavioral or neurologic symptoms.

### Histological analysis of disc in two groups

According to the histological grading scale, the discs of two groups were categorized as normal, moderately degenerated, and severely degenerated at all tested time points (**Tables 1 and 2**). In stabbed group, the moderately degenerated discs (7-11 points, 5.5 ± 2 weeks (mean ± SD)) were observed in all the five rats at 4 weeks and three of the five rats at 8 weeks, while the severely degenerated discs (12-15 points, 16.33 ± 6.76 weeks (mean ± SD)) were observed in two of the five rats at 8 weeks, and all the ten rats at 16 and 24 weeks. Therefore, the histologic score was progressively higher with the increase of the time post-stab. However, in control group, the AF was characteristically well organized with lamellar sheets of collagen. The NP demonstrated a mix of large vacuolated (notochordal) cells and smaller chondrocyte-like cells. Thus, normal discs (5-6 points, 12 ± 7.6 weeks (mean ± SD)) were observed in all the five rats at 4, 8, 16 and 24 weeks in control group, and their histologic score was not obviously changed along the increase of the time. Such histologic aspects were also observed in the preoperatively sacrificed four rats (**Figure 2**). Therefore, the discs of control group and preoperatively sacrificed rats were categorized into normal histologic grade. However, in stab group, no notochordal cells were detected in the NP, which was gradually occupied by disorganized hypocellular fibro-cartilaginous tissue at 24 weeks (**Figure 2**). In the stab specimens, increasing lamellar disorganization was present in the inner half of the AF, together with inward bulging of the inner annulus and tears. The border between the AF

## Relationship between MRI and histology in disc degeneration

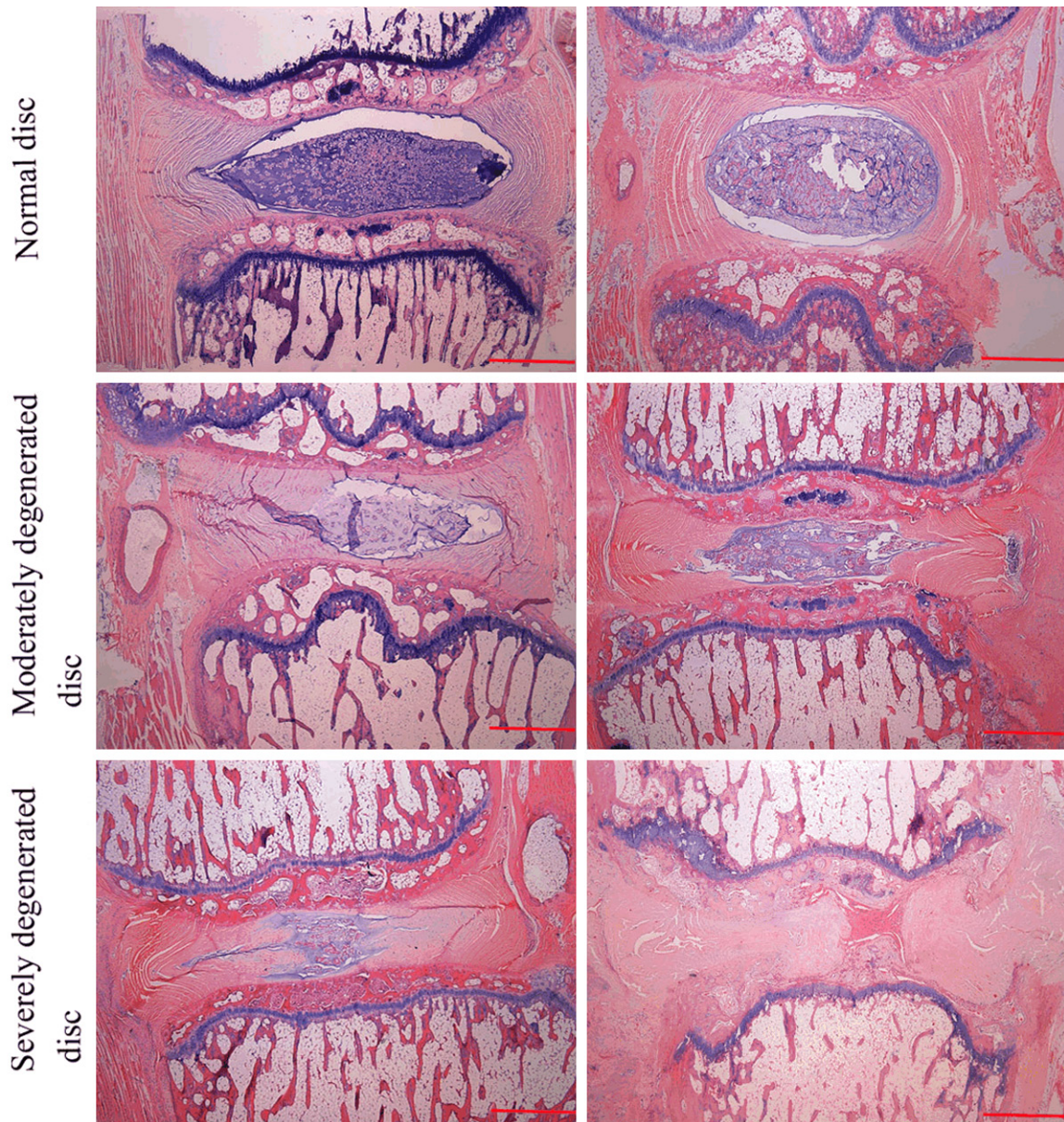


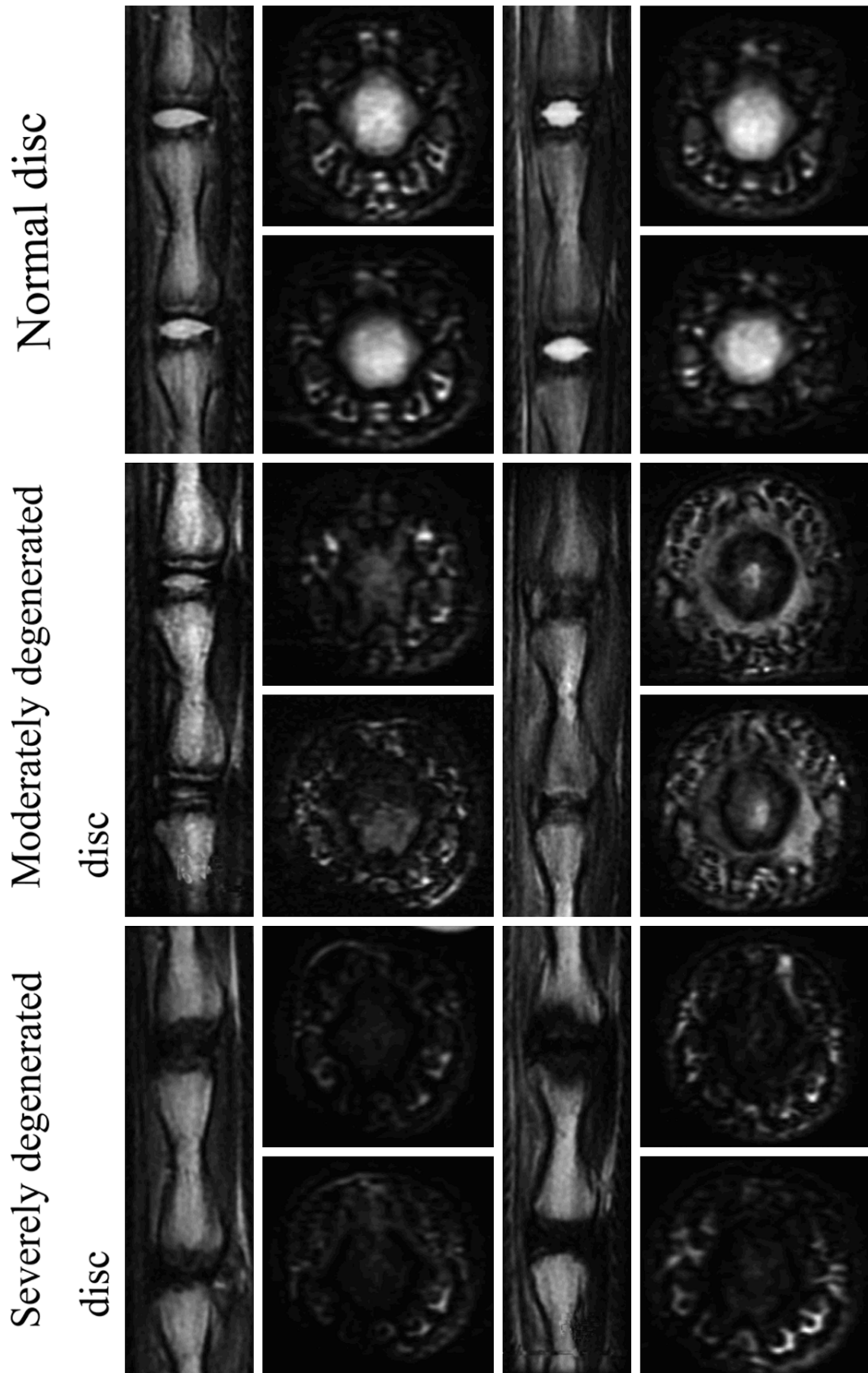
**Figure 2.** Representative H&E staining of disc samples from normal, moderately degenerated and severely degenerated groups. The bar: 1 mm.

and NP became progressively interrupted, and NP extrusion into the AF intralamellar space was evident in 4-week specimens. The nuclear cells became large, rounded, grouped into clusters and separated by dense areas of proteoglycan matrix (**Figure 2**). Furthermore, the inward bulging of AF and the extrusion of the NP tissue could be detected by MRI imaging (**Figure 3**). In addition, the histologic score of stab group discs (moderately and severely degenerated discs) was significantly higher than in the control group (**Table 2**,  $P < 0.001$ ), and

the histologic score of severely degenerated discs was significantly higher than in moderately degenerated discs (**Table 2**,  $P < 0.001$ ).

### *MRI assessment of disc in two groups*

Representative serial MRI scans of the coccygeal spine of one rat were shown in **Figure 3**, consisting of T2-weighted, midsagittal plane images obtained before surgery and 4, 8, 12, and 24 weeks after stab of the Co7/Co8 and Co8/Co9 discs. In midsagittal and axial plane



## Relationship between MRI and histology in disc degeneration

**Figure 3.** Representative T2 MRI scans of disc samples from normal, moderately degenerated and severely degenerated groups.

**Table 3.** Changes in T2-weighted intensity and MRI index in control and needle-stabbed discs at various time points after injury in 3-month-old rats

Factor	Group (No. of discs)	4 W	8 W	16 W	24 W
T2 density	Control group (10)	5279.9 ± 737.88	4846.41 ± 826.58	5044.31 ± 893.68	4546.41 ± 722.58
	Stab group (10)	2824.04 ± 474.83†	1773.19 ± 698.1†	855.97 ± 348.17†	476.42 ± 200.72†
MRI index	Control group (10)	17941.1 ± 2012.21	15915.61 ± 2714.48	18275.53 ± 2864.21	14021.13 ± 2187.38
	Stab group (10)	9014.33 ± 1515.65†	5181.26 ± 2019.84†	1914.8 ± 625.84†	1289.66 ± 457.61†

Values are expressed as the mean ± SD. The MRI index = area of interest in NP × corresponding image T2 intensity. †P < 0.001 compared with the control disc at the same time point.

**Table 4.** Changes in T2-weighted intensity, area, MRI index and histologic score in normal, moderately degenerated and severely degenerated discs after injury in 3-month-old rats

Group (No. of discs)	T2 intensity	Area (mm <sup>2</sup> )	MRI index	Histologic score (5-16)
Control group (40)	4935.26 ± 789.67	3.35 ± 0.19	16515.38 ± 2317.25	5.5 ± 0.51
Moderately degenerated disc (16)	2824.04 ± 474.83†,‡	2.99 ± 0.12†,‡	8440.85 ± 1995.82†,‡	8 ± 1.9†,‡
Severely degenerated disc (24)	651.89 ± 195.48†	2.47 ± 0.21†	1610.18 ± 658.27†	13.7 ± 1.08†

Values are expressed as the mean ± SD. The MRI index = area of interest in NP × corresponding image T2 intensity. †P < 0.001 compared with the control disc at the same time point. ‡P < 0.001 moderately degenerated disc compared with severely degenerated disc.

images, the bright NP area in the control disc remained relatively consistent over the 24-week period. However, progressive loss in both signal intensities and MRI indices was obvious in discs stabbed by 20-gauge needles. **Table 3** listed the mean and standard deviation of average T2-weighted signal intensity and MRI index of the stabbed (Co7/Co8 and Co8/Co9) discs at 4, 8, 12, and 24 weeks post stab from MRI scans of 5 rats at every time points post stab. Both T2 signal intensity and MRI index in stab group exhibited significant decrease from 4 weeks post stab, compared with control group (P < 0.001). **Table 4** listed the mean and standard deviation of NP area, average T2-weighted signal intensity, and MRI index of control and needle-stabbed discs in 3-month-old rats. All three MRI outcome measurements in the normal discs from control group were significantly higher than in moderately and severely degenerated discs (**Table 4**, P < 0.001). Similarly, all three MRI outcome measurements in the moderately degenerated discs were significantly higher than in severely degenerated discs (**Table 4**, P < 0.001).

### Discussion

Colloidal substances are the main body of extracellular matrix (ECM) in the NP. The main

contents of ECM are type II collagen fibers, proteoglycans and water [24]. While there are only a few cellular components in the NP, notochord and cartilage-like cells are the main two cell types [25]. For MRI T2 imaging, the long T2 value is due to the higher water content of tissue, and the signal intensity of NP is determined by T2 values, therefore the normal NP shows a long T2 value and high signal intensity [26, 27]. The IDD is mainly due to the imbalance between the degradation and synthesis of ECM, and the T2 values would become shorter as the water content of the NP gradually decreased. Such pathological changes provide a basic for MRI diagnosis of IDD, and MRI is a highly specific and sensitive method in the diagnosis of IDD [28, 29].

For correlation analysis, the relative signal intensity of NP calculated by a complex mathematical formula was compared with pathological stage of IDD. Marinelli et al. concluded that T2 signal intensity of IVD annulus fibrosus and nucleus pulposus correlated strongly with water content and weakly with proteoglycan content [30]. Although a moderate positive correlation between T2 intensity and water content was noted for the NP tissue samples, there was no significant correlation between T2 intensity and proteoglycan content [31].

## Relationship between MRI and histology in disc degeneration

However, the correlation between MRI measurements and pathological grade of IDD remains unclear.

In this study, the area and average T2 intensity of ROI were multiplied to get MRI index [22]. We found that with the increase of IDD severity, the T2 intensity and MRI index accordingly decreased, and there was a significant correlation between IDD severity with T2 signal intensity or MRI index. MRI data suggested that a slow and progressive degenerative process had begun by 4 weeks. The moderate degenerated discs were harvested from five rats of 4 weeks and three rats of 8 weeks post stab, while the severe degenerated discs were harvested from two rats of 8 weeks and ten rats from 16 and 24 weeks post stab. Especially at 16 and 24 weeks post stab, all the discs had severe IDD. The ultimate malformation of disc morphology was consistent with the earlier reduction of T2 intensity over time, which did not recover by itself.

The present study has several limitations. First, the characteristics of caudal discs are different between rat and human. Therefore, it is not proper to use the Pfirrmann grading system for MRI data, which might make the results more objective. Second, MRI processing method used in our study could be improved by implementing automated techniques to analyze the disc, rather than depending on an observer to identify the ROI. Third, although H&E staining is able to show a variety of different tissue structures, specialized techniques may be needed to demonstrate certain structural features in this model. For example, Kim et al. analyzed safranin O-stained sections to observe the formation of fibrocartilage using polarized light microscopy in the aging rabbit disc [32].

In summary, this study demonstrated that 20-gauge needle puncture into the tail disc in rat induces a slow and progressive disc degeneration process without spontaneous recovery. MRI T2 signal intensity and MRI index could be used for quantitative analysis of normal discs, degenerated discs and the level of degenerated discs in this rat model. According to histological outcome measurements, MRI could provide a convenient, non-invasive, reproducible, and cost-effective option to monitor the progression of the IDD and evaluate new modalities for treating disc degeneration.

### Acknowledgements

This study was partly supported by grants from the Nature Science Foundation (LQ-14H060-002, LY14H060004 and LY13H180006) and Science and Technology Foundation (2016C-33151) and the health foundation (201614-6428) of Zhejiang Province and the National Nature Science Foundation of China (81401822 and 81572177).

### Disclosure of conflict of interest

None.

**Address correspondence to:** Chengzhen Liang, Department of Orthopedics, 2<sup>nd</sup> Affiliated Hospital, School of Medicine, Zhejiang University, #88 Jiefang Road, Hangzhou 310009, Zhejiang, China. Tel: +86 571 8778 35715; Fax: +86 571 8778 3577; E-mail: liangchengzhen@zju.edu.cn

### References

- [1] Katz JN. Lumbar disc disorders and low-back pain: socioeconomic factors and consequences. *J Bone Joint Surg Am* 2006; 88 Suppl 2: 21-24.
- [2] Chuanting L, Qingzheng W, Wenfeng X, Yiyi H and Bin Z. 3.0T MRI tractography of lumbar nerve roots in disc herniation. *Acta Radiol* 2014; 55: 969-975.
- [3] Adams MA and Roughley PJ. What is intervertebral disc degeneration, and what causes it? *Spine (Phila Pa 1976)* 2006; 31: 2151-2161.
- [4] Roughley PJ. Biology of intervertebral disc aging and degeneration: involvement of the extracellular matrix. *Spine (Phila Pa 1976)* 2004; 29: 2691-2699.
- [5] Liang C, Li H, Tao Y, Zhou X, Li F, Chen G and Chen Q. Responses of human adipose-derived mesenchymal stem cells to chemical microenvironment of the intervertebral disc. *J Transl Med* 2012; 10: 49.
- [6] Liang C, Li H, Tao Y, Shen C, Li F, Shi Z, Han B and Chen Q. New hypothesis of chronic back pain: low pH promotes nerve ingrowth into damaged intervertebral disks. *Acta Anaesthesiol Scand* 2013; 57: 271-277.
- [7] Richardson SM, Doyle P, Minogue BM, Gnaniingham K and Hoyland JA. Increased expression of matrix metalloproteinase-10, nerve growth factor and substance P in the painful degenerate intervertebral disc. *Arthritis Res Ther* 2009; 11: R126.
- [8] Cui M, Wan Y, Anderson DG, Shen FH, Leo BM, Laurencin CT, Balian G and Li X. Mouse growth and differentiation factor-5 protein and DNA

## Relationship between MRI and histology in disc degeneration

- therapy potentiates intervertebral disc cell aggregation and chondrogenic gene expression. *Spine J* 2008; 8: 287-295.
- [9] Driscoll TP, Nakasone RH, Szczesny SE, Elliott DM and Mauck RL. Biaxial mechanics and inter-lamellar shearing of stem-cell seeded electrospun angle-ply laminates for annulus fibrosus tissue engineering. *J Orthop Res* 2013; 31: 864-870.
- [10] Lee KI, Moon SH, Kim H, Kwon UH, Kim HJ, Park SN, Suh H, Lee HM, Kim HS, Chun HJ, Kwon IK and Jang JW. Tissue engineering of the intervertebral disc with cultured nucleus pulposus cells using atelocollagen scaffold and growth factors. *Spine (Phila Pa 1976)* 2012; 37: 452-458.
- [11] Gilbertson L, Ahn SH, Teng PN, Studer RK, Niyibizi C and Kang JD. The effects of recombinant human bone morphogenetic protein-2, recombinant human bone morphogenetic protein-12, and adenoviral bone morphogenetic protein-12 on matrix synthesis in human annulus fibrosis and nucleus pulposus cells. *Spine J* 2008; 8: 449-456.
- [12] Sowa G, Westrick E, Pacek C, Coelho P, Patel D, Vadala G, Georgescu H, Vo N, Studer R and Kang J. In vitro and in vivo testing of a novel regulatory system for gene therapy for intervertebral disc degeneration. *Spine (Phila Pa 1976)* 2011; 36: E623-628.
- [13] Liang CZ, Li H, Tao YQ, Peng LH, Gao JQ, Wu JJ, Li FC, Hua JM and Chen QX. Dual release of dexamethasone and transforming growth factor beta3 from polymeric microspheres for the stem cell matrix accumulation in a rat disc degeneration model. *Acta Biomater* 2013; 9: 9423-33.
- [14] Kwon YJ. A minimally invasive rabbit model of progressive and reproducible disc degeneration confirmed by radiology, gene expression, and histology. *J Korean Neurosurg Soc* 2013; 53: 323-330.
- [15] Liang CZ, Li H, Tao YQ, Peng LH, Gao JQ, Wu JJ, Li FC, Hua JM and Chen QX. Dual release of dexamethasone and TGF-beta3 from polymeric microspheres for stem cell matrix accumulation in a rat disc degeneration model. *Acta Biomater* 2013; 9: 9423-9433.
- [16] Lipson SJ and Muir H. Experimental intervertebral disc degeneration: morphologic and proteoglycan changes over time. *Arthritis Rheum* 1981; 24: 12-21.
- [17] Lipson SJ and Muir H. 1980 Volvo award in basic science. Proteoglycans in experimental intervertebral disc degeneration. *Spine (Phila Pa 1976)* 1981; 6: 194-210.
- [18] Masuda K, Aota Y, Muehleman C, Imai Y, Okuma M, Thonar EJ, Andersson GB and An HS. A novel rabbit model of mild, reproducible disc degeneration by an anulus needle puncture: correlation between the degree of disc injury and radiological and histological appearances of disc degeneration. *Spine (Phila Pa 1976)* 2005; 30: 5-14.
- [19] Han B, Zhu K, Li FC, Xiao YX, Feng J, Shi ZL, Lin M, Wang J and Chen QX. A simple disc degeneration model induced by percutaneous needle puncture in the rat tail. *Spine (Phila Pa 1976)* 2008; 33: 1925-1934.
- [20] Zhang H, La Marca F, Hollister SJ, Goldstein SA and Lin CY. Developing consistently reproducible intervertebral disc degeneration at rat caudal spine by using needle puncture. *J Neurosurg Spine* 2009; 10: 522-530.
- [21] Schiebler ML, Camerino VJ, Fallon MD, Zlatkin MB, Grenier N and Kressel HY. In vivo and ex vivo magnetic resonance imaging evaluation of early disc degeneration with histopathologic correlation. *Spine (Phila Pa 1976)* 1991; 16: 635-640.
- [22] Sobajima S, Kompel JF, Kim JS, Wallach CJ, Robertson DD, Vogt MT, Kang JD and Gilbertson LG. A slowly progressive and reproducible animal model of intervertebral disc degeneration characterized by MRI, X-ray, and histology. *Spine (Phila Pa 1976)* 2005; 30: 15-24.
- [23] Mao HJ, Chen QX, Han B, Li FC, Feng J, Shi ZL, Lin M and Wang J. The effect of injection volume on disc degeneration in a rat tail model. *Spine (Phila Pa 1976)* 2011; 36: E1062-1069.
- [24] Hughes SP, Freemont AJ, Hukins DW, McGregor AH and Roberts S. The pathogenesis of degeneration of the intervertebral disc and emerging therapies in the management of back pain. *J Bone Joint Surg Br* 2012; 94: 1298-1304.
- [25] Adams MA and Dolan P. Intervertebral disc degeneration: evidence for two distinct phenotypes. *J Anat* 2012; 221: 497-506.
- [26] Samartzis D, Karppinen J, Chan D, Luk KD and Cheung KM. The association of lumbar intervertebral disc degeneration on magnetic resonance imaging with body mass index in overweight and obese adults: a population-based study. *Arthritis Rheum* 2012; 64: 1488-1496.
- [27] Zobel BB, Vadala G, Del Vescovo R, Battisti S, Martina FM, Stellato L, Leoncini E, Borthakur A and Denaro V. T1rho magnetic resonance imaging quantification of early lumbar intervertebral disc degeneration in healthy young adults. *Spine (Phila Pa 1976)* 2012; 37: 1224-1230.
- [28] Moon CH, Jacobs L, Kim JH, Sowa G, Vo N, Kang J and Bae KT. Part 2: Quantitative proton T2 and sodium magnetic resonance imaging to assess intervertebral disc degeneration in a rabbit model. *Spine (Phila Pa 1976)* 2012; 37: E1113-1119.
- [29] Bowles RD, Gebhard HH, Dyke JP, Ballon DJ, Tomasino A, Cunningham ME, Hartl R and

## Relationship between MRI and histology in disc degeneration

- Bonassar LJ. Image-based tissue engineering of a total intervertebral disc implant for restoration of function to the rat lumbar spine. *NMR Biomed* 2012; 25: 443-451.
- [30] Marinelli NL, Haughton VM, Munoz A and Anderson PA. T2 relaxation times of intervertebral disc tissue correlated with water content and proteoglycan content. *Spine (Phila Pa 1976)* 2009; 34: 520-524.
- [31] Weidenbaum M, Foster RJ, Best BA, Saed-Nejad F, Nickoloff E, Newhouse J, Ratcliffe A and Mow VC. Correlating magnetic resonance imaging with the biochemical content of the normal human intervertebral disc. *J Orthop Res* 1992; 10: 552-561.
- [32] Kim KW, Lim TH, Kim JG, Jeong ST, Masuda K and An HS. The origin of chondrocytes in the nucleus pulposus and histologic findings associated with the transition of a notochordal nucleus pulposus to a fibrocartilaginous nucleus pulposus in intact rabbit intervertebral discs. *Spine (Phila Pa 1976)* 2003; 28: 982-990.